Influence of crosslinking on micromechanical characteristics of liquid silicone rubber. Numerical simulations of microindentation process

G. Zamfirova[1*], S. Cherneva[2], V. Gaydarov[1], T. Vladkova[3]

[1] *Todor Kableshkov University of Transport, 158 Geo Milev Str., BG-1576 Sofia, Bulgaria*
[2] *Institute of Mechanics, Bulgarian Academy of Sciences, Acad. G. Bonchev Str., Bl. 4, BG-1113 Sofia, Bulgaria*
[3] *University of Chemical Technology and Metallurgy, 8 Kliment Ohridski Blvd., BG-1756 Sofia, Bulgaria*

Mechanical properties of three samples from liquid silicone rubber were investigated by means of microindentation experiments and finite-element simulations. The experimental and numerical load-displacement curves were compared and showed good coincidence. One of the aims of present work was seeking of correlation between some standard classical mechanical characteristics and parameters obtained by micro- and nanoindentation. The influence of the crosslinking on mechanical properties was investigated as well. Moreover parameters describing plastic behavior of investigated materials (such as yield strength, distribution of equivalent Von Mises stress in investigated materials during the process of microindentation, distribution of the equivalent plastic strain after unloading), which aren't possible to be obtained only by means of microindentaion experiments, were determined by means of numerical simulations.

Key words: liquid silicone rubber, microindentation, mechanical properties, numerical simulations, finite-element method

INTRODUCTION

Investigations of mechanical properties of polymer materials are very important, because they give information about the technological and exploitation characteristics of the materials and their applicability for different purposes. From classical mechanical investigations (for example tensile test) at constant deformation rate or creep test at constant load, or whatever static or dynamic mechanical experiment, we could not obtain direct information about the supramolecular structure because the standard mechanical approaches evaluate the material as a whole, including all types of its defects. Unfortunately, the complexity of the molecular and supramolecular structure of the polymers as well as the structural imperfections, macro-, micro- and nanodefects, the relations between standard mechanical properties and structure are difficult to be determined and interpreted. The increasing information and experience in the field of micromechanical methods give opportunity to consider the micro- and nano-mechanical investigations as adequate tools for elucidating some structural peculiarities of polymeric materials.

The aim of present work is to look for correlation between some standard classical mechanical characteristics and parameters obtained by micro- and nanoindentation. This could be considered as a link between structural peculiarities of the sample and its macromechanical behaviour.

EXPERIMENTAL

Materials

Three silicone rubber samples with different crosslinking were investigated. They are commercial product of KCC Corporation, Korea from the group Liquid Silicone Rubber (LSR) consisting mainly of silicone polymer and fumed silica. Liquid silicone rubber is cured automatically in liquid injection molding machines.

The components are supplied at a regular ratio. This mixed compound is measured by volume using some mechanical tools in the injection unit. Finally heat curing is done very quickly in a hot mold. After the fixed cure time, de-molding is completed and the cured articles are taken from the mold. In addition, the cure system includes curing by platunum catalyst so therefore, it is physiologically inert.

Mechanical properties of investigated silicon rubber materials, provided by producer are shown in the Table 1.

It is obviously from Table 1 that from sample 1 to sample 3 Shore hardness increases and elongation

Table 1. Mechanical properties of the three types of silicone rubber provided by the manufacturer

Sample	Hardness (Shore A)	Tensile strength (MPa)	Elongation (%)	Tear strength (N/mm)
1. SL7240	39	8	750	36
2. SL7250	49	10	600	27
3. SL7270	67	9	400	40

* To whom all correspondence should be sent:
gzamfirova@mail.bg

decreases. There is inverse proportion between Shore hardness and elongation which is usually attributed to increasing the cross-linking. So the increasing the sample number means the increasing of the degree of cross-linking. Tensile strength is the maximum stress that a material can withstand while being stretched or pulled before failing or breaking.

Tear strength is a specific characteristic which is widely used when study mechanical behavior of rubber or textile materials. It is defined as a maximum stress obtained from stress-strain experiment divided to sample thickness. There is some similarity between the tear strength and yield strength what concerns to initiation of plastic deformation but loading test and sample geometry are different.

Tensile strength and tear strength are not influenced linearly by degree of crosslinking.

Methods

This investigation was carried out predominantly by method known as a depth-sensing indentation (DSI) or instrumented indentation testing (IIT). The method consists of recording by a testing device at a constant loading speed the magnitude of the force as a function of penetration depth for each point on the loading (or unloading). Large amount of mechanical parameters are determined using indentation curves, obtained by above mentioned method:

— Dynamic hardness (DH)

$$HD = \frac{aF}{h^2},\qquad(1)$$

where (F) is the value of the instant load at loading and unloading testing regime, $(a = 3.8584)$ is a constant which depends on the shape of the indenter and (h) is an indentation depth. This characteristic reveals how the material responds to plastic, elastic and viscoelastic deformation during the test.

— Martens hardness (HMs) is determined from the slope (m) of the increasing load-displacement curve in the 50% ÷ 90% Fmax interval and characterizes the material resistance of penetration:

$$HMs = \frac{1}{26.43m^2}.\qquad(2)$$

This characteristic has similar physical sense as dynamic hardness, but characterizes material properties at maximum indentation depth and constant load.

— Indentation hardness (H_{it}) is determined using Oliver-Pharr approximation method and measure re-

sistance to permanent deformation.

$$H_{it} = \frac{F_{max}}{24.50h_c^2},\qquad(3)$$

where (h_c) is the depth of contact of the indenter with the test sample.

— Indentation Elastic Modulus (E_{it}) is calculated from unloading part of the load-displacement curve:

$$\frac{1}{E_r} = \frac{1 - v_s^2}{E_{it}} + \frac{1 - v_i^2}{E_i},\qquad(4)$$

where (E_r) is the experimentally converted elastic modulus, based on indentation contact, (v_s) is the Poisson's ratio of specimen, whereas (E_i) and (v_i) are the Young's modulus and Poisson's ratio for indenter, respectively.

— Indentation creep (C_{it}) which is a relative change in the indentation depth at constant test force is calculated as:

$$C_{it} = \frac{h_2 - h_2}{h_1},\qquad(5)$$

where (h_1) and (h_2) are indentation depths at the beginning and at the end of the creep measurement.

— Elastic part of indentation work (η_{it}) is determined from the areas under loaded and unloaded part of the load- unload test $(W = \int Pdh)$:

$$\eta_{it} = \frac{W_{el}}{W_{el} - W_{pl}}.\qquad(6)$$

Vickers hardness, HV*, is obtained as a function of computed indentation hardness. Its direct measurement from the diagonal of the residual imprint was impossible because of the absence of residual imprint.

For more comprehensive characterization of the samples, we apply hybrid experimental-numerical approach to the indentation experiment, which combines microindentation experiments with numerical simulations by means of finite-element method (FEM). The combination of the indentation experiment and its numerical simulation has a number of advantages, because enables determination of some valuable mechanical properties (yield strength, distribution of equivalent Von Mises stress, distribution of the equivalent plastic and elastic strain in the zone under indenter and etc.).

The experimental conditions, which we used for conducting microindentation tests, are following:
— First mode is loading- unloading;
• Indenter is Vickers diamond pyramid with angle of 136°;

- Loading rate of 0.0250 mN/s;
- Maximum load – 0.8 mN;
- Minimum load – 0.020 mN;
- Holding time after unloading 0 s;
- Poisson's ratio 0.47;
- Indenter Poisson's ratio of 0.07;
- Indenter Modulus of 1140 GPa

Measurements have been carried out at room temperature. At least 30 indentations for each sample have been made and average value and the mean square error have been calculated, which could be considered as an indicator of the microstructural heterogeneity of the samples.

Also a measuring by the mode loading-holding at maximum load-unloading with holding time 60 s for determining the indentation creep has been made. All other experimental conditions are the same.

The equilibrium swelling and effective crosslink density were determined by Dogadkin-Tarrasova's method using toluene as a swelling agent [1].

Numerical simulations of microindentation process

Boundary value problem. The boundary value problem is defined under the following assumptions:

- The indentation process is quasistatic;
- The deformable axisymmetric specimen is composed by an isotropic linear elastic-plastic with linear hardening material;
- Normally indenter's material is very hard (usually this is a material with elastic modulus $\approx 10^3$ GPa). For that reason it is accepted, that the indenter can be modelled as a rigid body;
- The friction forces in the contact area are neglected;
- No stress-strain prehistory is taken into account.

The equation of motion of the deformable body is:

$$\sigma_{ij,j} = 0, \qquad (7)$$

where σ_{ij} is the Cauchy stress tensor. Because of the axial symmetry the boundary condition on G_1 is (see Fig. 1):

$$u_{y|G_1} = 0. \qquad (8)$$

The deformable body is imposed on a rigid base and this gives the following boundary condition on the surface G_5:

$$u_{x_{|G_5}} = 0. \qquad (9)$$

The indenter I penetrates from the side of contact surface G_2 with a prescribed velocity v_I. The depth
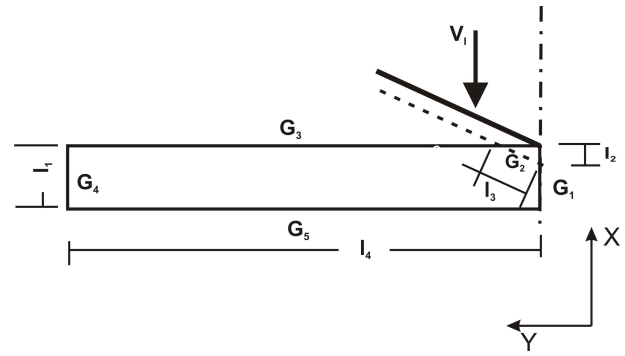

Fig. 1. Scheme of the boundary value problem.

of the contact zone l_2 during the deformation process changes. On the contact zone the velocity is given as:

$$v_{|G_2} = v_I, \qquad (10)$$

Material model. The material model used in present work is elastic-plastic with linear hardening. The model involves the following material parameters: Young's modulus, Poisson's ratio, yield strength, strength coefficient.

The strain tensor ε_{ij} is used to describe the deformation in a material point belonging to the investigated material:

$$\varepsilon_{ij} = \frac{1}{2}\left(u_{i,j} + u_{j,i}\right), \qquad (11)$$

where $\{u_1, u_2, u_3\}$ is the displacement vector of the material point at position $\{x_1, x_2, x_3\}$ in the reference configuration. The material model applied to investigated materials is described below.

The total strain tensor ε_{ij} is a sum of the elastic strain tensor ε_{ij}^e and the plastic strain tensor ε_{ij}^p:

$$\varepsilon_{ij} = \varepsilon_{ij}^e + \varepsilon_{ij}^p. \qquad (12)$$

The elastic strain tensor is related to the stress tensor through Hooke's law:

$$\varepsilon_{ij}^e = \frac{1+\nu}{E}\delta_{ij} + \frac{1-2\nu}{3E}\sigma_{kl}\delta_{kl}\delta_{ij}, \qquad (13)$$

where E is the Young's modulus and ν is the Poisson's ratio of the particular material.

Following the von Mises yield criterion, yielding occurs in a point when the next validates:

$$F\left(\sigma_{ij}, \overline{\varepsilon}^p\right) \equiv \frac{3}{2}s_{ij}s_{ij} - \sigma_p^2\left(\overline{\varepsilon}^p\right) = 0, \qquad (14)$$

where s_{ij} is deviator of the stresses and $\overline{\varepsilon}^p$ is the equivalent plastic strain. The flow stress σ_p of the material depends on the accumulated plastic strain

435

and the value of the initial yield stress $\sigma_p^{0.2}$. If the initial yield stress is exceeded, the material starts to show plastic yielding. It is assumed that the material is isotropic with linear hardening behavior. In this case the evolution of σ_p during plastic deformation is given by:

$$\sigma_p\left(\overline{\varepsilon}^p\right) = \sigma_p^{0.2} + K\overline{\varepsilon}^p, \qquad (15)$$

where K is the strength coefficient.

The accumulated equivalent plastic strain is given by:

$$\overline{\varepsilon}^p = \int_0^t \sqrt{\frac{2}{3}\dot{\varepsilon}_{ij}^p \dot{\varepsilon}_{ij}^p} dt \qquad (16)$$

According to the associated plastic flow rule, the plastic strain rate is given by

$$\dot{\varepsilon}_{ij}^p = \dot{\lambda}\frac{\partial F}{\partial \sigma_{ij}}, \qquad (17)$$

where $\dot{\lambda}$ is the plastic multiplier.

Indentation test procedure modelling. The process of indenter penetration and separation from the specimen is simulated as a contact problem. It is evident from the experiment that the deformation caused by the indenter is located in a small area around the indenter. For that reason a boundary value problem is defined in a cylindrical domain around the indenter's tip with sufficiently large radius compared to the size of the indenter. The radius is chosen in such way that the deformation due to the penetration vanishes at the lateral and the bottom of the considered cylindrical domain.

The friction forces on the contact surface are neglected. The experiment that has to be simulated numerically is a microindentation, where the indenter is a tetrahedral Vickers pyramid with tip angle 136°. Because of geometrical symmetry, the considered domain can be reduced and only one fourth of the whole domain is used for solving the boundary value problem. Often the problem is simplified by substituting the geometry of the Vickers pyramid with the circular cone with an angle of 70.3° between the axis and the generatrix. Such approach has been applied for example in [2–4]. In this case the problem can be considered as an axisymmetric one. The geometry of the 2D model is shown in Fig. 1.

Numerical simulations. The above described process of microindentation is modelled numerically. The finite- element model has been developed using the finite-element code MSC.MARC [5]. The boundary value problem is based on the model described in Sections 2.3.1, 2.3.2 and 2.3.3. The geometry of the domain is given on Fig. 1: l_1=0.5 mm, l_4=2 mm.

The relation between l_3 and l_4 is $\frac{l_3}{l_4} = \frac{1}{20}$. In this way the influence of boundary conditions on the numerical solution is avoided [6].

As initial values for the material properties of investigated materials, we used data taken from the certificates of these materials, available at the Web page of the producer (values are shown in Table 1) and literature [7]. They are given in second column of Table 3. For the modelling process of microindentation, 3 series of finite element simulations with 3600 four-nodes isoparametric finite elements with full integration have been performed (Fig. 2). The experimental and calculated load-displacement curves were then compared. In this way we performed a trial-error procedure in order to obtain the material parameter set that gives the best fit to the experimental data. They are shown on third column of Table 3.
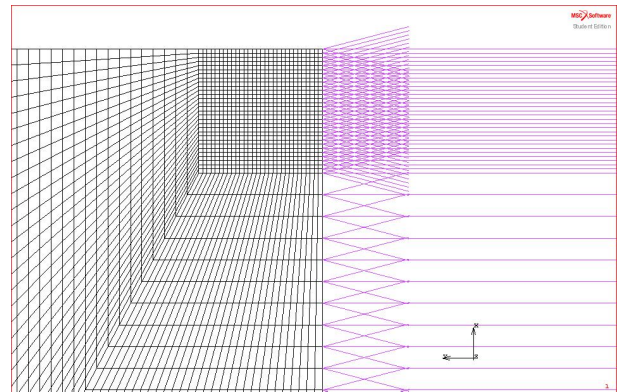

Fig. 2. Enlargement part from FE mesh for the 2D model around the indenter.

RESULTS AND DISCUSSIONS

Fig. 3 shows experimental indentation curves for three silicon rubber samples with different degrees of crosslinking. The loading and unloading parts of indentation curves are close to each other, which is typical for materials with high elasticity. Indentation curve for sample 2 is the most inclined, i.e. it posses the smallest hardness. This can be seen directly from the diagram in the Fig.4, which illustrate the values of dynamic hardness (DH), Martens hardness (MHs), indentation hardness (H_{it}) and Vickers hardness (HV*).

It is obviously from Figs. 3 and 4 that all microhardness characteristics are not directly dependent on
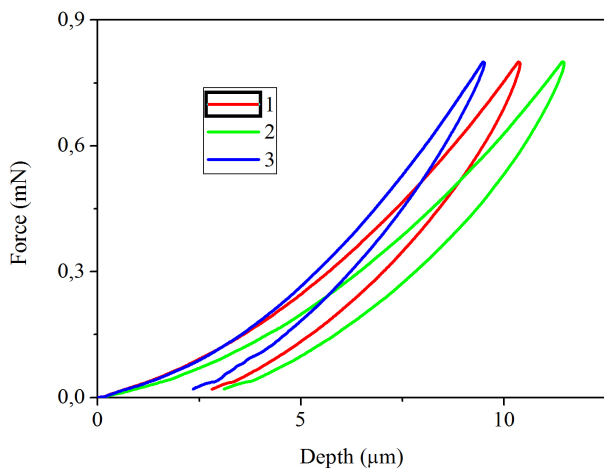
Fig. 3. Experimental indentation curves for three silicon rubber samples with different degrees of crosslinking.
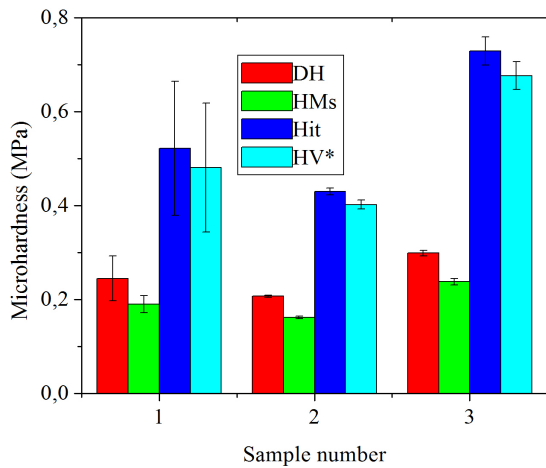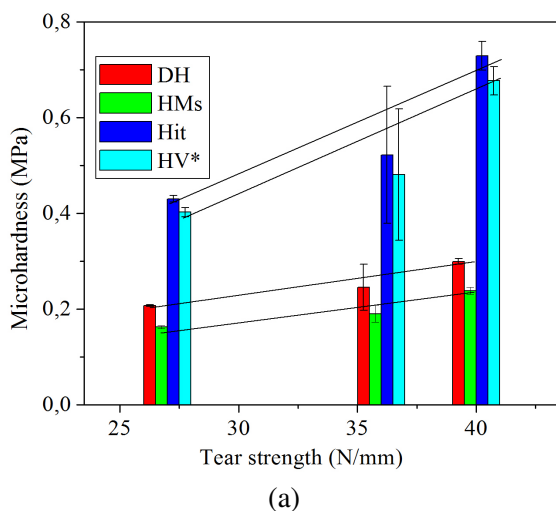

Fig. 4. All hardness characteristics for the three samples.

degree of crosslinking. The same is valid for indentation modulus and elastic part of the indentation work.

No relation has been found between the microindentation parameters and tensile strength, which could be expected because microindentation parameters characterize the local mechanical properties while the tensile strength is statistically measured parameter. It depends not only on material properties but also on existing of macro-defects in loaded zone, which become stress concentrators and increase until the break of the material.

The dependence of hardness characteristics from tear strength is shown on Fig. 5a. It is observed almost linear dependence. Moreover both characteristics which are related to resistance against plastic deformation (H_{it} and HV*) are more sensitive to tear strength. Dynamic and Martens hardnesses which characterize the resistance against total deformation, including elastic and plastic deformation components are less sensitive to tear strength. Also indentation modulus linearly depends on the tear strength (Fig. 5b).

As we mentioned in the experimental part it is physically unreasonable to look for some relation between microindentation parameters and parameters like yield strength and tensile strength, because they basically depend on macro defects. But when measure the indentation characteristic there is one indirect indicator for existence of macro-defects- it is the results scattering, i.e. the big error in measurements. Percentage errors vs. tensile strength are plotted in
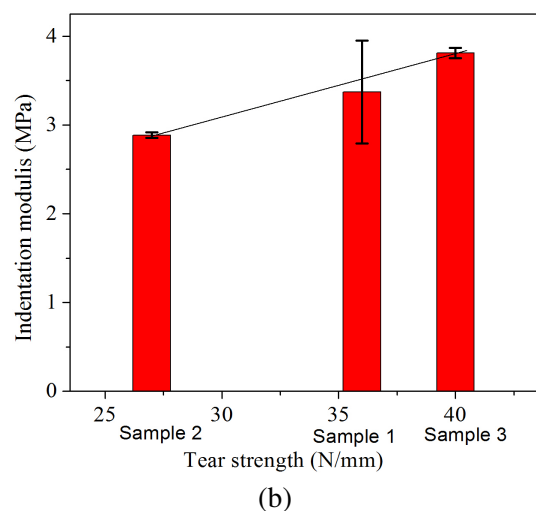

| (a) | (b) |

Fig. 5. All experimentally obtained microhardness characteristics (a) and indentation moduli (b) for the three investigated samples as a function of tear strength.
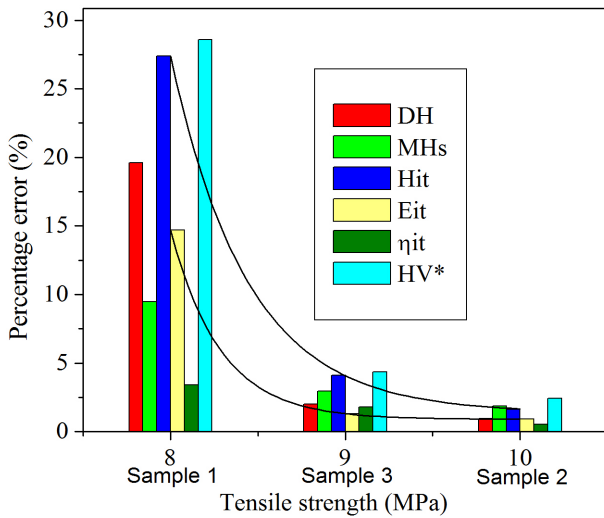
Fig. 6. Relation between percentage error for all microindentation characteristics and tensile strength.
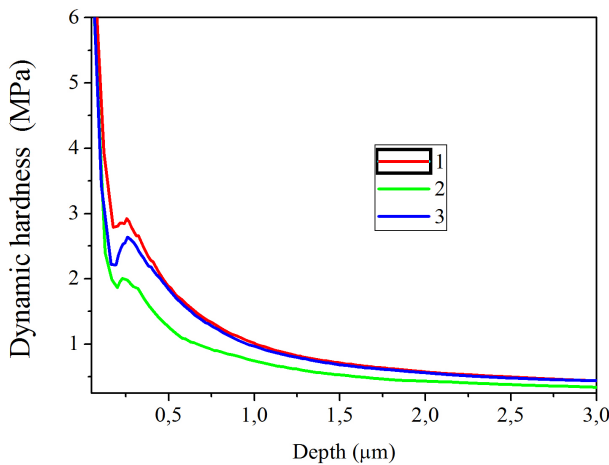

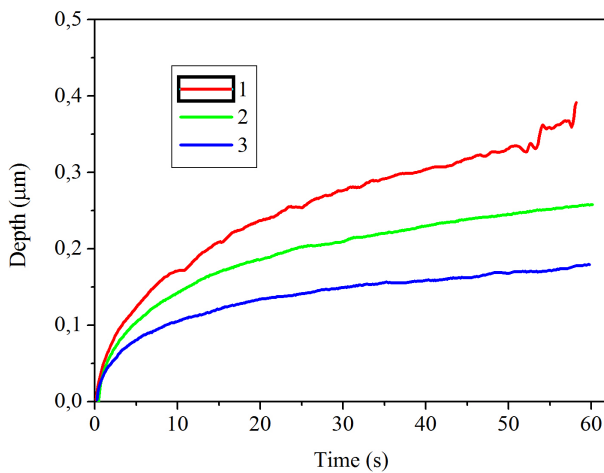Fig. 7. Microindentation profiles.

Fig. 8. Creep curves.

Fig. 6. Sample 1 is the most inhomogeneous one and it has small tensile strength. Sample 2 is very homogeneous and has the highest tensile strength. The dependence has exponential decreasing character.

Fig. 7 shows microhardness profiles i.e. how the dynamic hardness changes in the depth of the specimen. It should be emphasized that the hardness values do not indicate the resultant hardness of the material exactly at this depth but incorporate the properties of all surface layers up to that depth. Moreover at very small depths (in this case less than about 4 μm) the hardness increases sharply, which by now has no precise and unambiguous physical explanation. It's called "scale factor" or "size factor". In this zone some structural heterogeneity could be seen near to the surface, but it is difficult to make some comment in this not well studied area.

The results for equilibrium swelling and effective crosslink density, which were determined by means of Dogadkin-Tarrasova's method are shown in Table 2. It is observed almost linear dependence between effective crosslink density and Shore hardness of investigated samples from liquid silicone rubber.

Table 2. Values for equilibrium swelling and effective crosslink density, determined by Dogadkin-Tarrasova's method

Sample	Equilibrium swelling Q	Effective crosslink density n.10^{-19}/cm^3
1. SL7240	3.6	0.66
2. SL7250	3.1	0.91
3. SL7270	2.8	1.36

Fig. 8 shows the creep curves i.e. increasing of the depth with time in constant load. The creep is more pronounced for sample 1 which has less crosslinking and decreases with increasing of crosslinking. This is logical because denser lattice means bigger resistance to time-dependent deformation. The creep curve for specimen 1 is not smooth, confirming its low homogeneity.

Comparison between experimental and numerical load-displacements curves is shown in Fig. 9 and in the Table 3.

The distribution of equivalent Von Mises stress in investigated materials during the modelled process of microindentation, as well as the distribution of the equivalent plastic strain after unloading are shown in Figs. 10-12. These figures show sink-in of material

Table 3. Initial values for numerical simulations (taken from literature and manufacturer certificates) and material parameter set, which gives the best fit with experimental results

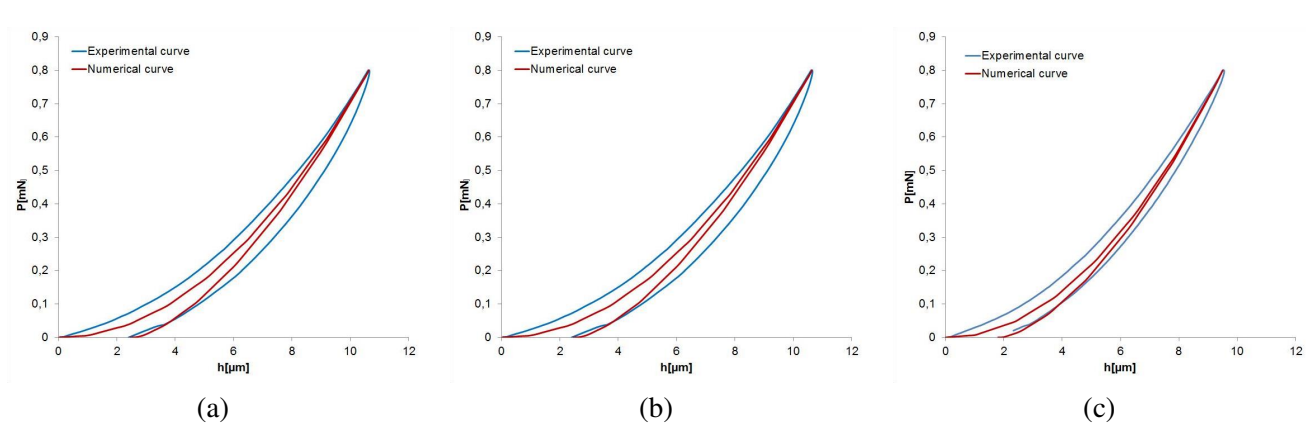| Material	Initial values					Best fit			
	σ_p (MPa)	K (-)	E_{it} (MPa)	ν (-)		σ_p (MPa)	K (-)	E_{it} (MPa)	ν (-)
1	3.73	2.41	3.37	0.47		0.426	2.41	2.77	0.47
2	3.73	2.41	2.89	0.47		0.400	2.41	2.35	0.47
3	3.73	2.41	3.81	0.47		0.600	2.41	3.45	0.47

(a) (b) (c)

Fig. 9. Comparison between experimental and numerical load-displacement curves for material 1 (a), 2 (b) and 3 (c).
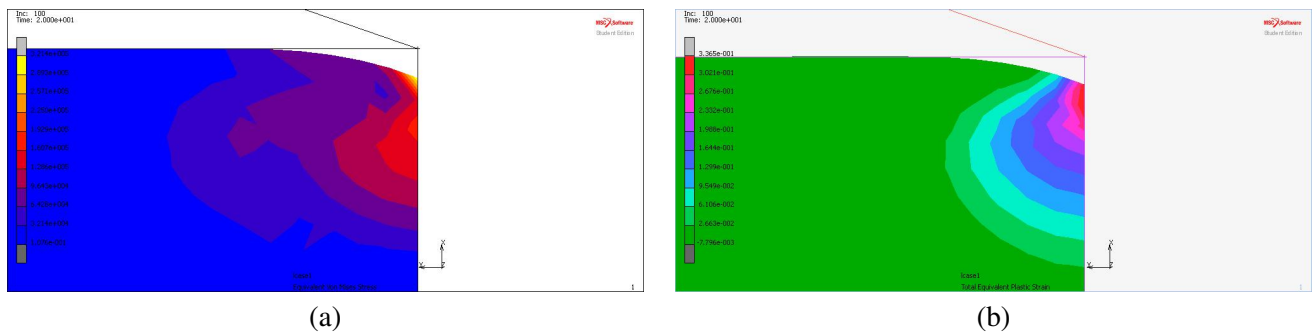

(a) (b)

Fig. 10. Distribution of equivalent Von Mises stress (a) and the equivalent plastic strain (b) in material 1.

(a) (b)

Fig. 11. Distribution of equivalent Von Mises stress (a) and the equivalent plastic strain (b) in material 2.

439

(a)　　　　　　　　　　　　　　　　　(b)

Fig. 12. Distribution of equivalent Von Mises stress (a) and the equivalent plastic strain (b) in material 3.

around indenter imprint, which could be taken into account only by means of numerical simulations and could be one of the reasons for explaining the difference between experimental and numerical values of elastic modulus.

CONCLUSIONS

In present work we have investigated the influence of crosslinking on mechanical properties of three liquid silicon rubber samples. We established:

- Increasing in the degree of crosslinking confirm that elasticity has no direct influence on the microhardness characteristics because they are fully (H_{it}, HV*) or partially (DH, HMs) dependent from the plastic deformation (irreversible slippage of the macromolecules);
- Only creep curves are influenced by the crosslinking. The creep is more pronounced for the sample which has less crosslinking and decreases with increasing of crosslinking;
- There is a linear dependence between all microhardness characteristics and indentation modulus on one hand and tear strength and yield strength on the other hand. So this good correlation between these micro- and macro- characteristics indicates that both are affected in the same way by the structural features of the rubber, but crosslinking is not a main decisive factor;
- The scattering of the results in microindentation experiment, respectively magnitude of the experimental error can be regarded as an indirect indicator of the magnitude of tensile strength.

Three series of numerical simulations were realized by means of the finite-element method and the results were compared with experimental results from microindentation measurements. In this way, a trial-error procedure was performed in order to obtain the material parameter set that gives the best fit to the experimental data. The constitutive model used in the finite-element model of microindentation process is based on the Von Mises yield criterion in combination with a linear hardening law. Moreover figures 10-12 show sink-in of material around indenter imprint, which could be taken into account only by means of numerical simulations. Numerical simulations by means of finite-element method, which we realized, gave us additional information about mechanical properties of investigated materials, which is impossible to obtain by means of microindentation experiment only. Moreover this hybrid experimental-numerical approach save money and time for preparing of test samples and realizing conventional experiments in order to obtain plastic behavior of investigated materials.

REFERENCES

[1] B. A. Dogadkin, Z. N. Tarasova and A. S. Linkin, *J. Vsesojusnovo Chimicheskova Obstestva Imeni Mendeleeva (USSR)* **13**, 87 (1968).

[2] J. C. Hay, A. Bolshakov and G. M. Pharr, *J. Mater. Res.* **14**, 2296–2305 (1999).

[3] G. M. Pharr and A. Bolshakov, *J. Mater. Res.* **17**, 2660–2671 (2002).

[4] A. Bolshakov and G.M. Pharr, "Inaccuracies in Sneddon's solution for elastic indentation by a rigid cone and their implications for nanoindentation data analysis" in *Proceedings of the Conference "Spring Meeting of the Materials Research Society"* CONF-960401-16, Materials Research Society, San Francisco, USA, May 1996.

[5] MSC. Software Corporation, USA, MSC.MARC User's Guide, 2013.

[6] S. Cherneva and R. Iankov, "Investigation on the influence of the boundary conditions by simulation with finite element method of microindentation process" in *Proceedings of the Thirty Sixth Spring Conference of the Union of Bulgarian Mathematicians*, St. Konstantin & Elena Resort, Varna, Bulgaria, 2007, pp. 197–202.

[7] Materials and Coatings for Medical Devices: Cardiovascular (book), ASM Materials for Medical Devices Database Committee, ASM International, USA, November 2009, pp. 297-303.

ВЛИЯНИЕ НА СТЕПЕНТА НА ОМРЕЖВАНЕ ВЪРХУ МИКРОМЕХАНИЧНИТЕ ХАРАКТЕРИСТИКИ. СИМУЛАЦИЯ НА МИКРОИНДЕНТАЦИОННИЯ ПРОЦЕС

Г. Замфирова[1], С. Чернева[2], В. Гайдаров[1], Т. Владкова[3]

[1] *ВТУ "Тодор Каблешков", ул. "Гео Милев" №158, 1574 София, България*
[2] *Институт по механика, Българска академия на науките, ул. "Акад. Г. Бончев" блок 4, 1113 София, България*
[3] *Химикотехнологичен и металургичен университет, бул. "Св. Кл. Охридски" №8, 1756 София, България*

(Резюме)

Изследвани са образци от силиконов каучук с различна степен на омрежване чрез метода на контролирано проникване на индентора (Depth Sensing Indentation (DSI)). От експериментално получените индентационни криви са определени редица микроиндентационни характеристики:

— микротвърдост по Викерс (HV*);

— индентационна твърдост (Hit);

— Мартенсова твърдост (HMs);

— динамична твърдост (HMV);

— модул на еластичност (E);

— отношение между еластичната и пластична компонента на деформацията;

— криви на пълзене;

— промяна на динамичната твърдост в дълбочина на образеца и др.

Установено е, че степента на омрежване няма директно влияние върху микротвърдостните величини и модула, защото те са свързани изцяло (Hit, HV*) или частично (HMV, HMs) с пластичните деформации. Но възвратимата деформация, която е сума от мигновенната Хуковска деформация и времезависимата вискоеластична деформация се влияят от гъстотата на мрежата. Затова степента на омрежване оказва почти линейно увеличение на работата, необходима за еластична деформация, и намаляване на дълбочината на проникване при режим на пълзене.

Направена е симулация по метода на крайните елементи, чрез която са определени:

— разпределение на еквивалентните напрежения на фон Мизес;

— разпределение на пластичните деформации за сложното напрегнато състояние под индентора в натоварено състояние;

— границата на пластично течение и нейната зависимост от степента на омрежване.

Така този хибрид на експериментално-числен подход спестява голямо количество материал за изготвяне на опитни образци, средства и време за подготовката на пробите за тестване и реализиране на допълнителни експерименти.